HHS Public Access

Author manuscript

Nat Mater. Author manuscript; available in PMC 2018 April 02.

Published in final edited form as:

Nat Mater. 2017 December ; 16(12): 1243–1251. doi:10.1038/nmat4993.

Mechanical confinement regulates cartilage matrix formation by chondrocytes

Hong-pyo Lee[1], **Luo Gu**[2,3], **David J. Mooney**[2,3], **Marc E. Levenston**[1], and **Ovijit Chaudhuri**[1,†]

[1]Department of Mechanical Engineering, Stanford University, Stanford, CA 94305, USA

[2]School of Engineering and Applied Sciences, Harvard University, Cambridge, MA 02138, USA

[3]Wyss Institute for Biologically Inspired Engineering, Harvard University, Cambridge MA 02138, USA

Abstract

Cartilage tissue equivalents formed from hydrogels containing chondrocytes could provide a solution for replacing damaged cartilage. Previous approaches have often utilized elastic hydrogels. However, elastic stresses may restrict cartilage matrix formation and alter the chondrocyte phenotype. Here we investigated the use of viscoelastic hydrogels, in which stresses are relaxed over time and which exhibit creep, for 3D culture of chondrocytes. We found that faster relaxation promoted a striking increase in the volume of interconnected cartilage matrix formed by chondrocytes. In slower relaxing gels, restriction of cell volume expansion by elastic stresses led to increased secretion of IL-1β, which in turn drove strong up-regulation of genes associated with cartilage degradation and cell death. As no cell adhesion ligands are presented by the hydrogels, these results reveal cell sensing of cell volume confinement as an adhesion-independent mechanism of mechanotransduction in 3D culture, and highlight stress relaxation as a key design parameter for cartilage tissue engineering.

Osteoarthritis, a chronic disease characterized by degeneration of articular cartilage, is a major cause of severe disability. As articular cartilage is avascular and has a limited intrinsic healing capacity, even small defects of articular cartilage can deteriorate and lead to osteoarthritis[1,2]. Current clinical treatments for repairing cartilage defects include autologous chondrocyte implantation (ACI)[3], matrix-induced autologous chondrocyte

†Correspondence to: chaudhuri@stanford.edu.
Correspondence and requests for materials should be addressed to O.C.

COMPETING FINANCIAL INTERESTS

The authors declare no competing financial interests.

AUTHOR CONTRIBUTIONS

HL, ML, and OC designed the experiments. HL conducted all experiments and analyzed the data. LG and DJM contributed to the materials design and materials. HL and OC wrote the manuscript.

DATA AVAILABILITY

The datasets generated during and/or analyzed during the current study are available from the corresponding author on reasonable request.

Supplementary information is available in the online version of the paper.

implantation (MACI)[4], micro fracture[5], and allografts[6]. However, each of these treatments have had limited success over the long-term. Formation of fibrocartilage instead of articular cartilage is a well-known issue associated with ACI[7], MACI[7], and microfracture[8], with fibrocartilage impairing joint function, while allografts carry the risk of disease transmission from the donor[6].

Cartilage tissue equivalents derived from hydrogels containing chondrocytes could provide a solution for repairing or replacing damaged cartilage[9–11]. Various hydrogels, such as poly-ethylene glycol[12], agarose[13], alginate[9], hyaluronic acid[14], and collagen[15] have been used for 3D culture of chondrocytes, and some aspects of cartilage tissue have been replicated in these hydrogels[15]. However, proliferation of chondrocytes can be limited[16] and cartilage matrix deposition often occurs only immediately adjacent to the cells leading to islands of cartilage matrix within a sea of hydrogel[15,17]. The source of limited proliferation and cartilage matrix formation may be the elastic nature of hydrogels typically used, as elastic stresses in these hydrogels would be expected to resist cell proliferation and the formation of cartilage matrix[12,15]. Recent studies have found that viscoelastic hydrogels, in which stresses are relaxed over time, promote spreading and proliferation of adherent cells, and formation of an interconnected bone matrix by osteogenically differentiated MSCs in 3D culture[18,19]. While there has been extensive study of the impact of hydrogel stiffness or elasticity on cartilage matrix formation by chondrocytes[20–22], the impact of hydrogel stress relaxation, related to viscosity and creep, on chondrocytes remains unknown. Here we test whether viscoelastic hydrogels that exhibit fast stress relaxation could provide a microenvironment that is more conducive to cartilage matrix formation by chondrocytes.

Faster relaxation or greater creep promotes enhanced formation of cartilage matrix

To assess the impact of viscoelastic properties on chondrocytes, we utilized alginate hydrogels, in which the rate of stress relaxation or creep could be modulated independent of initial elastic modulus, swelling, and matrix degradability. Alginate is a polysaccharide that does not present any cell-adhesion ligands for cells to bind to, and is not degradable by mammalian enzymes[23]. Alginate can be crosslinked into a 3D hydrogel with divalent cations such as calcium, and these hydrogels have been widely used for 3D culture of cells, including chondrocytes[24–26]. Ionic crosslinking results in viscoelastic hydrogels[27,28], as the weak ionic crosslinks can unbind under stress or strain, allowing the hydrogel polymer matrix to flow[28]. Material viscoelasticity is often characterized using a stress relaxation test, in which a constant strain is applied to a material, and the resulting stress, corresponding to the resistance to deformation, is measured over time[28]. Several approaches were used to vary the stress relaxation rate in alginate hydrogels. As in a recent study[18], hydrogels were formed using alginate with an average molecular weight of 280 kDa, 70 kDa, or 35 kDa, but the same overall concentration of 2% wt/vol alginate (Fig 1a, b, Supplementary Table 1). Calcium crosslinking concentrations were adjusted so that the initial elastic moduli of the gels were constant (Fig. 1c). It was found that hydrogels formed from lower molecular weight alginate exhibited faster stress relaxation. Further, covalent coupling of short PEG spacers to the low molecular weight alginate (35kDa) led to hydrogels with even faster stress

relaxation in the gel. Finally, mixtures of batches of alginate with different average molecular weights led to formation of hydrogels with intermediate levels of stress relaxation. Specifically, the time ($\tau_{1/2}$) when the stress is relaxed to half of the initial value ranged from ~2 hour to ~1 minute (Fig. 1a, b), with a constant initial elastic modulus of hydrogels of ~3kPa (Fig. 1c). Stress relaxation tests were conducted in unconfined compression, as relaxation of ionically crosslinked alginate hydrogels under compression was previously found to occur due to ionic crosslinker unbinding and polymer flow, and not water migration out of the gels[18,28]. When stress relaxation tests were conducted in shear, a similar ordering and range in relaxation times was observed and the loss tangent, a measure of viscosity that is defined as the ratio of loss modulus to storage modulus, was a monotonic function of stress relaxation, confirming this interpretation (Fig. 1d, Supplementary Fig. 1a–c). In addition to stress relaxation tests, viscoelasticity of alginate hydrogels was also characterized using creep tests in which a constant shear stress is applied to a material, and the resulting strain, corresponding to the extent of deformation, is measured over time (Fig. 1e). The creep time ($\tau_{3/2}$), defined as the time at which the strain reaches 150% of its original value under a constant stress, exhibited a similar range and a strong linear correlation with the timescales for stress relaxation (Fig. 1f, Supplementary Fig. 1d). These confirm that stress relaxation, creep, and the loss tangent can all be used interchangeably to describe the viscoelasticity of these alginate hydrogels. Alginate polymer concentration was maintained at 2% wt/vol in all gels, and all gels were found to be mechanically stable, exhibiting negligible loss of the dry polymer mass and no detectable change in swelling over three weeks (Fig. 1g, h).

Using this set of hydrogels, we investigated the impact of hydrogel relaxation on cartilage matrix formation by chondrocytes. Juvenile bovine chondrocytes were encapsulated in hydrogels with various stress relaxation rates and an initial modulus of ~3kPa. Formation of cartilage matrix by chondrocytes was assessed first with immunohistochemical staining for type II collagen and aggrecan, critical components of cartilage matrix, after three weeks of culture. In slow relaxing hydrogels ($\tau_{1/2}$~ 2h), deposition of type II collagen and aggrecan was restricted to the region only immediately adjacent to the cells (Fig. 2a). This matches the results previously reported in non-degradable elastic hydrogels[20]. Strikingly, as the rate of stress relaxation or creep was enhanced, greater areas of type-II collagen and aggrecan deposition and a more interconnected cartilage matrix were observed in the faster relaxing gels (Fig. 2a). In addition, in the fast relaxing gels, chondrocytes formed canonical pericellular matrices (PCM), as indicated by staining for type VI collagen, and exhibited bean-shaped morphologies resembling those of chondrocytes in PCM in normal hyaline cartilage[29] (Fig. 2b, Supplementary Fig. 2, 3a). A quantitative assessment of cartilage matrix area formed per chondrocyte confirmed that faster relaxation led to a wider area of cartilage matrix formed per chondrocyte (Fig. 2c). As immunohistochemical stainings were done on random sections of the gels, greater area of cartilage matrix measured in the sections corresponds to greater volume of cartilage matrix in the 3D constructs. As the alginate hydrogels used in this study are nanoporous with negligible degradation and surround the chondrocytes, displacement of hydrogels must accompany cartilage matrix formation outside of the cells. Using fluorescent beads to track gel strains, displacement was observed in fast relaxing hydrogels but not in slow relaxing hydrogels (Supplementary Fig. 4). Next,

amounts of both collagen and sulfated glycosaminoglycan (sGAG), another major component of cartilage matrix, deposited by chondrocytes were quantitatively assessed at various timepoints. Chondrocytes were found to deposit significantly higher levels of both collagen and sGAG in hydrogels with faster stress relaxation (Fig. 2d–e). Interestingly, while the amount of cartilage matrix area formed per cell was a monotonic function of stress relaxation, both normalized amounts of collagen and sGAG to DNA in gels were similar in the faster relaxing gels, or gels with stress relaxation times ranging from $\tau_{1/2}$ = 965 seconds to 63 seconds (Supplementary Fig. 5). Macroscopically, the hydrogel constructs exhibited increased opacity with faster relaxation, as would be expected for increased production of cartilage matrix (Supplementary Fig. 3b).

As previous work has implicated hydrogel stiffness in mediating cartilage matrix formation[20,21,30], we next examined how altered hydrogel stiffness regulated the effect of relaxation. In hydrogels with an initial elastic modulus of 20 kPa, trends similar to those in 3 kPa gels were observed, with faster relaxation leading to greater areas of type-II collagen and aggrecan deposition as well as higher quantities of secreted collagen and sGAG (Supplementary Fig. 6, 7, 8). Interestingly, the impact of stiffness on cartilage matrix formation was diminished in hydrogels with faster relaxation. In slow relaxing gels, production of both sGAGs and collagen was significantly higher in the softer hydrogels relative to the stiffer hydrogels, but this difference substantially decreased in gels with faster stress relaxation (Fig. 2f–g). Importantly, a comparison of the impact of calcium concentration on cartilage matrix formation in all the gel formulations indicates that these effects are due to mechanics and not calcium concentration (Supplementary Fig. 9). These findings indicate that the impact of stiffness on cartilage matrix is affected by hydrogel viscoelasticity.

Hydrogel relaxation regulates the chondrogenic phenotype

Next, we established the impact of hydrogel relaxation on chondrocyte number. The construct DNA content, related to the number of chondrocytes, exhibited a strong correlation with the rate of stress relaxation in hydrogels with an initial elastic modulus of 3 kPa (Fig. 3a, Supplementary Fig. 8c). The amount of DNA decreased in hydrogels with slower stress relaxation, corresponding to a decrease in cell number. As changes in cell number arise from a combination of cell proliferation and cell death, cell proliferation and death were quantitatively assessed in the gels. Proliferation of chondrocytes, indicated by nuclear staining of Ki-67, was enhanced in gels with faster stress relaxation and suppressed in gels with slower stress relaxation after 7 days in culture (Fig. 3b–c). Conversely, cell death, indicated by levels of lactate dehydrogenase (LDH) released into the media, was significantly diminished in gels with faster stress relaxation after 7 days in culture (Fig. 3d). A similar trend was observed in hydrogels at a higher stiffness (Supplementary Fig. 10). These findings indicate that faster relaxation enhanced chondrocyte proliferation and inhibited cell death.

To assess the chondrocyte response to altered hydrogel relaxation, we measured the expression of anabolic genes, which are involved in cartilage matrix synthesis, and catabolic genes, which are involved in cartilage matrix degradation. Faster relaxation led to significant

up-regulation of anabolic genes, such as type II collagen and aggrecan, after 7 days of culture (Fig. 3e–f, Supplementary Fig 11, 12) relative to those cultured in slower relaxing gels. While there was a slight increase in expression of type I collagen, known to be associated with fibrocartilage, with faster relaxation, no type I collagen was detected in any gel in immunohistochemical stainings (Supplementary Fig 13). In contrast, expression of genes ADAMTS4 and MMP13, whose products are involved in cartilage matrix turnover as well as catabolism of cartilage matrix, was strongly up-regulated in chondrocytes cultured in slower relaxing gels for 7 or 21 days relative to those cultured in fast relaxing gels (Fig. 3h–i, Supplementary Fig. 12d–e). Expression levels of SOX9, a key transcription factor for chondrocytes[31], did not exhibit any significant correlation with stress relaxation at day 7 (Fig. 3g). Therefore, hydrogel relaxation regulates the chondrocytic phenotype, with faster relaxation promoting the matrix-forming functions of chondrocytes independent of SOX9 expression, and slower relaxation inducing a gene expression profile associated with matrix degradation.

The impact of hydrogel relaxation is mediated through IL-1β secretion

After finding a strong impact of hydrogel relaxation on chondrocyte fate and function, we investigated the molecular mechanism underlying this effect. The phenomena of increased cell death and strongly up-regulated catabolic gene expression, observed in chondrocytes encapsulated in slow relaxing hydrogels, are also observed during osteoarthritis[32]. Previous studies have identified the cytokine interleukin-1β (IL-1β), produced by immune cells and chondrocytes, as a major driver of osteoarthritis progression, finding that IL-1β secretion induces strong up-regulation of catabolic gene expression and massive apoptosis of chondrocytes in osteoarthritic cartilage[33,34]. Intriguingly, we found a strong increase in expression of IL-1β and elevated levels of IL-1β protein released into the media in chondrocytes cultured in hydrogels with slower relaxation after 7 days, indicating that slow relaxation activated IL-1β signaling (Fig. 4a–b). Up-regulated gene expression of IL-1β persisted after 3 weeks of culture in hydrogels with slow stress relaxation (Supplementary Fig. 12e). To test the role of IL-1β signaling in driving cell death and catabolic gene expression in slow relaxing hydrogels, IL-1β signaling was inhibited by blocking IL-1β receptor binding using the IL-1 receptor antagonist (IL-1Ra). Strikingly, inhibition of IL-1β signaling in chondrocytes cultured in hydrogels with slow relaxation resulted in reduced cell death and reduced expression of ADAMTS4 and MMP13 to levels approaching those of chondrocytes cultured in fast relaxing gels (Fig. 4c–e). These results demonstrate that the impact of hydrogel relaxation on chondrocyte death and catabolic gene expression is mediated through secretion of IL-1β produced by the chondrocytes.

Restriction of chondrocyte volume expansion induces IL-1β signaling

Next, we examined the physical mechanism through which hydrogel relaxation regulated IL-1β signaling. Notably, substantial differences in the size of chondrocytes in gels with different levels of stress relaxation were observed (Fig. 5a–b, Supplementary Fig. 14a–b). The size of single chondrocytes increased in faster relaxing gels, while cells in slower relaxing gels exhibited sizes similar to those of isolated primary chondrocytes prior to encapsulation. Time-lapse microscopy revealed that chondrocytes in fast relaxing gels

expanded over the 2 days following encapsulation, while chondrocytes in slow relaxing gels did not detectably expand over this time, despite substantial intracellular movements (Fig. 5c, Supplementary Videos 1–2). Importantly, the relationship between chondrocyte size and hydrogel stress relaxation was found to hold in other material systems. The size of single chondrocytes encapsulated in polyethylene glycol (PEG) hydrogels, which are elastic and exhibit negligible stress relaxation under compression, are similar to that found in the slow relaxing alginate hydrogels (Fig. 5d, Supplementary Fig. 15). Contrastingly, chondrocytes in agarose hydrogels, which are viscoelastic and exhibit stress relaxation comparable to the relaxation of the fast relaxing alginate hydrogels, exhibit sizes similar to those observed in the fast relaxing alginate hydrogels (Fig. 5d, Supplementary Fig. 15). Although extreme volume expansion of chondrocytes is associated with a hypertrophic phenotype[35], both gene expression and protein levels of type X collagen, a key marker of the hypertrophic phenotype, did not increase with faster stress relaxation (Supplementary Fig. 12f, 16). Further, the size of single chondrocytes in fast relaxing hydrogels was still significantly smaller than that of hypertrophic chondrocytes in the deep zone of cartilage (Supplementary Fig. 17). The size of chondrocytes cultured in slow relaxing hydrogels did not change when IL-1β signaling was inhibited by IL-1Ra, indicating that cell volume changes occurred upstream of IL-1β signaling (Fig. 5e). As the hydrogels do not present any cell adhesion motifs to promote cell signaling, together these results suggest the possibility that mechanical restriction of cell volume expansion in slow relaxing gels induces IL-1β signaling.

To test this possible mechanism, we directly assessed the impact of restricting cell volume expansion on IL-1β signaling in chondrocytes by using osmotic pressure to control chondrocyte volume. Chondrocytes were cultured in fast relaxing gels ($\tau_{1/2} \sim 478$s) for 7 days under a range of osmotic pressures. Osmotic pressure was modulated by adding different amounts of 400 Da PEG, an inert molecule, into the culture media. Increased osmotic pressure led to a decrease in cell size (Fig. 5d–e). The range of cell sizes resulting from variation of osmotic pressure in fast relaxing gels was similar to the range of cell sizes resulting from encapsulation of cells in hydrogels with different rate of stress relaxation. Proliferation of chondrocytes was found to decrease with higher osmotic pressure (Fig. 5f, g), while levels of cell death were found to increase with higher osmotic pressure (Fig. 5h). Further, strong up-regulation of IL-1β, ADAMTS4, and MMP13, as well as down-regulation of type II collagen, were observed in chondrocytes where cell volume expansion was inhibited by increased osmotic pressure (Fig. 5i–k, Supplementary Fig. 18). The impacts of altered cell volume on cell proliferation, cell death, and gene expression of IL-1β, ADAMTS4, and MMP13 when volume was modulated by varying hydrogel relaxation or osmotic pressure were quantitatively similar (Fig. 5l–p). As these represent two distinct approaches to modulating cell volume, the similar effects suggest that cell volume itself regulates these processes. Together, these findings indicate that spatial confinement against cell volume expansion by slower relaxing hydrogels restricted proliferation of chondrocytes and induced IL-1β signaling, cell death, and activation of a catabolic phenotype.

Outlook

This work establishes the role of hydrogel relaxation in mediating the ability of chondrocytes to form cartilage matrix. While there have been many mechanical property measurements of viscoelasticity in cartilage[36], chondrons[37,38], and chondrocytes[39,40], this mechanotransduction study examined how the matrix viscoelasticity impacts chondrocyte behavior. Previous studies have found limited proliferation and deposition of cartilage matrix by chondrocytes encapsulated in non-degradable or slowly-degrading hydrogels of PEG[12], agarose[13], alginate[41] and hyaluronic acid[22]. Similar behaviors were observed for chondrocytes encapsulated in slow relaxing alginate hydrogels. In contrast, in fast relaxing gels, chondrocytes proliferated, produced higher levels of key articular cartilage matrix proteins, and formed a more interconnected cartilage extracellular matrix containing PCM with bean-shaped chondrocytes. As the alginate hydrogels exhibited negligible degradation, underwent similar levels of gel swelling, and presented no cell-adhesion ligand binding sites to the cells, the observed response was attributed solely to the alteration in the mechanical property of viscoelasticity. Viscoelasticity in ionically crosslinked alginate hydrogels arises from ionic crosslinker unbinding followed by polymer matrix flow, and can be described by either stress relaxation, creep, or the loss tangent of the hydrogels. Interestingly, the timescale of stress relaxation of the fast relaxing alginate hydrogels of ~1s when tested in shear was similar to that of juvenile bovine cartilage tested in shear (Supplementary Fig. 19). Similarly, cartilage, chondron, and chondrocytes have been found to exhibit viscoelastic responses with characteristic timescales ranging from 0.5 – 10 seconds[36–40]. These indicate that the fast relaxing hydrogels may more closely mimic the viscoelasticity of the native cartilage microenvironment than the slow relaxing hydrogels.

Our results suggest two distinct mechanisms by which hydrogel relaxation mediates cartilage matrix formation and the chondrogenic phenotype in chondrocytes (Fig. 6). The first mechanism involves restriction of cell volume expansion following culture. We found that cell volume expansion was restricted in slower relaxing gels, and that this spatial confinement of cell volume activated IL-1β signaling, subsequently leading to increased cell death and catabolic gene expression. In contrast, in fast relaxing gels, elastic stresses resisting chondrocyte volume expansion are relaxed, allowing the cells to expand. This impact of stress relaxation on chondrocyte cell volume expansion in hydrogels for 3D culture was found in alginate hydrogels and confirmed in PEG and agarose hydrogels. The size of chondrocytes in fast relaxing hydrogels was larger than chondrocytes in mature hyaline cartilage[42], but smaller than hypertrophic chondrocytes in the deep zone of hyaline cartilage. We note that there could be multiple pathways by which chondrocytes can be induced to form large amounts cartilage matrix. Chondrocytes in cartilage tissue can actively remodel the surrounding microenvironment by using proteases to degrade the matrix, while the alginate hydrogels are not degradable by these proteases. Therefore, cartilage matrix forming activities and volume expansion may be different for chondrocytes in hyaline cartilage.

While previous studies have found the importance of volume regulation by chondrocytes in cartilage physiology[42–44], our work demonstrates that chondrocytes utilize changes in volume to sense the viscoelastic properties of their microenvironment. In adherent cells, it is

known that cells sense viscoelasticity through exerting traction forces at integrin-ECM ligand adhesions, gauging resistance to traction forces, and clustering ligands[18,45–48]. However, no integrin-binding cell adhesion ligands are present in the alginate hydrogels used here. Further, the volume expansion occurs over the first two days of culture, while cells are surrounded by the alginate hydrogel and before substantial amounts of cartilage matrix have been secreted. Therefore, the use of cell volume modulation to sense matrix viscoelasticity serves as an adhesion-independent mechanism of mechanotransduction in 3D culture. It is possible that adherent cells might use a combination of adhesion-independent and adhesion-mediated mechanisms to sense matrix viscoelasticity.

The second mechanism by which hydrogel relaxation mediates cartilage matrix formation and the chondrogenic phenotype in chondrocytes involves restriction of cartilage matrix deposition during the stage of cartilage matrix formation by chondrocytes. While the amounts of cartilage matrix component secreted by chondrocytes was similar in gels with stress relaxation times of 965s, 478s, and 63s, the amount of cartilage matrix volume formed per cell was a monotonically increasing function of stress relaxation rate, with a maximum volume of cartilage matrix formed in the fastest relaxing gels. In all of the hydrogels, chondrocytes are surrounded by a nanoporous hydrogel with negligible degradation, so that formation of extracellular cartilage matrix involves displacement of the surrounding hydrogel. In slow relaxing hydrogels, elastic stresses resist this displacement over long times. In faster relaxing gels, however, elastic stresses are dissipated, and chondrocytes form wide regions of cartilage matrix that become interconnected. A similar trend is observed in elastic hydrogels that are engineered to be degradable[12,49]. While it is difficult to compare these approaches, as degradation causes changes of other physical properties, the similarities broadly suggest that engineered degradation and faster relaxation represent two complementary approaches to improving cartilage matrix formation in hydrogels.

Previous studies have shown the importance of mechanical stiffness of hydrogels on regulation of chondrocyte function. The elastic moduli of the hydrogels used in these studies ranges from 2 kPa to 100 kPa[12,14,20,21], which is comparable to the moduli of chondrocyte PCM, ranging from 10 kPa to 75 kPa[29]. Enhanced stiffness in covalently crosslinked PEG based hydrogels, found to exhibit minimal stress relaxation here, restricted production of sGAG and collagens, distribution of cartilage matrix, and proliferation of chondrocytes[20,21]. However, our work revealed that the impact of stiffness was dependent on hydrogel relaxation. In our studies, the elastic modulus of the alginate hydrogels used was either 3 kPa or 20 kPa, falling within the range of moduli used in previous studies. A similar trend of reduced stiffness promoting cartilage matrix formation was only observed in the slow relaxing hydrogels, and the impact of stiffness was substantially diminished in hydrogels with fast relaxation.

The finding that IL-1β, a pro-inflammatory cytokine that plays a causal role in osteoarthritis pathogenesis, is involved in mediating the impact of hydrogel relaxation suggests a possible link to osteoarthritis. Previous studies proposed the role of either cartilage matrix stiffening[50] or volume expansion[43] in the initiation of osteoarthritis. We found that restricted cell expansion by a more elastic microenvironment induces IL-1β signaling. Therefore, these

results suggest a possible interplay between the biophysical properties of PCM and cell expansion during osteoarthritis progression.

METHODS

Alginate preparation

Sodium alginate with an average molecular weight of 280kDa (high-MW) was obtained for these studies (LF20/40, FMC Biopolymer). Molecular weight of alginate was modulated as has been described previously[18]. Briefly, Mid- or low-MW alginate was prepared by irradiating high-MW alginate with a 3 or 8 Mrad cobalt source, respectively. mid-MW alginate had an average molecular weight of 70 kDA and low-MW alginate had an average molecular weight of 35 kDa. Polyethylene glycol (PEG) coupled alginate was prepared following a previous protocol[18]. Briefly, one chain of low-MW alginate was covalently coupled to an average of two PEG-amine molecules (5 kDa, Laysan Bio) using carbodiimide chemistry. Specifically, at a pH of 6.5, 500 mg of alginate was dissolved in 50 ml of 0.1 M MES (2-(*N*-morpholino) ethanesulfonic acid, Sigma-Aldrich) buffer. Then 13.7 mg of Sulfo-NHS, 24.2 mg of EDC (*N*-(3-dimethylaminopropyl)-N^0 -ethylcarbodiimide hydrochloride, Sigma-Aldrich), and 295 mg of PEG-amine was mixed with the solution, and the reaction was allowed to proceed for 20 h. The resulting solution was dialyzed for three days in deionized water (molecular weight cutoff of 10 kDa). Finally, the product was purified with activated charcoal, sterile filtered, frozen and lyophilized.

Mechanical characterization

Unconfined compression tests were used to measure the initial elastic modulus of all hydrogels and juvenile cartilage and stress relaxation times of alginate gels and PEG hydrogels using a previously published method[18,28]. Gel and cartilage disks (6 mm in diameter, 2 mm thick) were equilibrated in DMEM for 24 h. First, a compressional deformation rate of 1 mm/min was applied to the gels, using an Instron 5848 material testing system with a 10N load cell, until a compressional strain of 15% was achieved. The initial elastic modulus was measured as the slope of the stress–strain curve between 5 and 10% strain. Subsequently, the 15% strain was held constant, while measuring stress over time. The stress relaxation time, $\tau_{1/2}$, was quantified as the time for which the initial stress of the gel was relaxed to half of its original value. Shear stress relaxation tests and creep tests were conducted using an AR-G2 stress-controlled rheometer (TA Instruments, DE). Samples were prepared for rheological analysis following a previously published method[51]. Alginate solution was directly deposited between two plates of the rheometer immediately after crosslinking, but before gelation. The storage modulus and the loss modulus were recorded over time to track gelation of the hydrogel solution. Once the hydrogels had fully gelled, as indicated by the storage and loss modulus reaching an equilibrium value, stress relaxation tests and creep tests were performed. The reported loss tangent was measured immediately prior to initiating the stress relaxation tests. The gel formed a 20 mm diameter disk with a thickness of ~1.0 mm. Mineral oil (Sigma, MO) was applied to the surface of hydrogels exposed to air to prevent the dehydration of hydrogel. The stress relaxation time was then measured over time for 20,000 seconds after a constant shear strain of 15 % strain was applied with a rise time of 0.1s. The creep time was measured over time for 10,000 seconds

after a constant shear stress of 100 Pa was applied with a rise time of 0.1s and the creep time, $\tau_{3/2}$, was quantified as the time for the strain to reach 150% of its initial value immediately following the application of stress. To prevent dehydration and slippage of cartilage disks (6mm in diameter, 2 mm thick) during shear stress relaxation tests, the cartilage disks were tightly held between a sandpaper covered base plate and a sandpaper covered top plate, and a custom plastic chamber was used to keep the edge of the disks immersed in Dulbecco's phosphate-buffered saline (DPBS, Invitrogen, CA). The initial elastic modulus of agarose hydrogels was measured using unconfined compression. However, stress relaxation of agarose hydrogels was measured in shear, since the stress relaxation of the agarose hydrogels was found to be highly sensitive to temperature and the rheometer provided precise control over temperature. Gelation of agarose hydrogels was conducted at 4 °C until the storage modulus and loss tangent reached an equilibrium value, and then stress relaxation tests were conducted at 37 °C.

Characterization of gel swelling and degradation

Characterization of gel swelling and degradation were conducted according to a previous method[18]. First, the wet weights of the hydrogels were measured after incubating hydrogels in cell culture media at 37 °C for either 1 or 21 days. Next, the hydrogels were frozen and lyophilized and then the dry weights of the lyophilized hydrogels were measured. The swelling ratio was calculated as the ratio of the wet weight to the dry weight.

Cell isolation

Chondrocyte isolation from bovine cartilage was conducted according to a previously published method[52]. Briefly, hyaline articular cartilage was harvested from a patellofemoral groove of a bovine leg. Bovine legs were purchased directly from a commercial vendor (Research 87, MA). The cartilage was then diced into ~1 mm^3 cubes, washed in Dulbecco's phosphate-buffered saline (DPBS, Invitrogen, CA), and digested for 24 hours at 37°C in standard Dulbecco's Modified Eagles Medium (DMEM, Invitrogen, CA) containing collagenase type II, type IV (Worthington Biochemical, NJ), and 1% Antibiotic-Antimycotic Solution (Corning, MA). After digestion, a 70 μm nylon filter was used to remove undigested cartilage. The filtered solution was centrifuged and washed twice in DPBS. The number of viable cells was determined using a VI-CELL counter (Beckman Coulter, IN). The chondrocytes were prepared for freezing by suspension in DMEM media with 50% fetal bovine serum (FBS, Invitrogen, CA) and 10% dimethyl sulfoxide (DMSO, Fisher, PA) and. The frozen cells were stored in liquid nitrogen until use in experiments.

Encapsulation of cells within hydrogels and 3D cell culture

Frozen bovine chondrocytes were thawed in a 37°C water bath, washed twice in DPBS, recounted, and used without further expansion. Cells were encapsulated in hydrogels as described previously[18]. First, cell solution was prepared by suspending the chondrocytes in serum-free DMEM at a final concentration of 100 million cells/ml, determined using a cell counter (VI-CELL, Beckman Coulter). Next, alginate solution and cell solution were each added to Luer lock syringes and then homogenously mixed, using a female–female Luer lock coupler (Value-plastics). Serum free DMEM containing various concentration of $CaSO_4$, in another Luer lock syringe, was then mixed with the cell-alginate solution. The

mixture was then deposited on a hydrophobic surface a glass plate, and then covered with another glass plate, with a 2 mm spacing between plates. The cell-alginate mixture was fully gelled for 45 min. For encapsulation of cells in PEG and agarose hydrogels, cells were resuspended at 100 million cells/mL in each hydrogel precursor solution. PEG hydrogel precursor solution consisted of 5% (w/v) poly (ethylene glycol diacrylate) (PEGDA,10kDa, Laysan Bio), and 0.05% w/v photoinitiator (Irgacure D 2959, Ciba Specialty Chemicals, NY) in DPBS. Agarose hydrogel precursor solution was composed of 4% (w/v) low melting temperature agarose (Cat# 50302, Lonza, Swiss) in DPBS heated to 60 °C. Both cell-hydrogel suspensions were deposited between two glass plates spaced 2mm apart. The agarose was allowed gel for 20mins on ice. The PEG was exposed to UV light (365 nm wavelength) following deposition between plates at 3 mW/m^2 for 5 minutes to induce gelation. Subsequently, all cell-hydrogels were punched out using a biopsy punch and immersed in growth medium. All hydrogels containing cells were cultured in the growth medium, which consisted of low glucose DMEM (Invitrogen, CA) containing 10% Fetal Bovine Serum (Invitrogen, CA), 0.1 mM nonessential amino acids (NEAA, GE, PA), 10mM HEPES (Invitrogen, CA), 0.05mg/ml L-ascorbic acid-2-phosphate (Sigma, MO), 1% Antibiotic-Antimycotic Solution (Corning, MA), and 1 mM calcium chloride (Sigma, MO). The medium was changed every 2–3 days during cell culture studies. For mechanical studies, the above procedure was conducted without mixing cells into the gels. For observing displacement of hydrogels, 0.2 μm fluorescent microspheres (Thermofisher, MA, Cat# F8811) were homogeneously mixed into the alginate solution at a final concentration of 20 million beads/μl before mixing cells with the alginate and gelation.

Immunohistochemistry

For immunohistochemistry, the samples for staining were prepared as described previously[18]. The hydrogel constructs were first fixed with 4% paraformaldehyde (Alfa Aesar, MA) for 60 min, and washed in PBS containing calcium (cPBS, GE, PA). The gels were placed in 30% sucrose (Fisher Scientific, PA) at 4°C for one day, and then incubated in OCT-sucrose, a mixture of 50% of 50% OCT (Tissue-Tek, Sakura, CA) and a 30% sucrose solution, for 5 hours. Gels were then embedded in OCT, frozen and sectioned. The sectioned samples for immunohistochemistry were prepared with a thickness of 30–80 μm using a cryostat (Leica CM1950), and processed using standard immunohistochemistry procedures. Sections were washed three times in DPBS, permeabilized with DPBS containing 0.5% Triton X-100 (Sigma, MO), and then blocked with blocking buffer that contained 1% bovine serum albumin (BSA, Sigma, MO), 10% Goat serum (Invitrogen, CA), 0.3M glycine (Fisher, PA) and 0.1% Triton X-100 in DPBS. The following antibodies/reagents were used for immunostaining: mouse monoclonal type I collagen antibody (Sigma, cat. #2456), aggrecan antibody (Abcam, cat. #3778), rabbit polyclonal type II collagen antibody (Abcam, cat. #34712), rabbit polyclonal type VI collagen antibody (Abcam, cat. #6588), rabbit polyclonal type X collagen antibody (Abcam, cat. #58632), Ki-67 antibody (Thermofisher, cat. #9106), Prolong Gold antifade reagent with DAPI (Invitrogen, CA), AF-488 Phalloidin to stain actin (Invitrogen, CA), Goat anti-Rabbit IgG AF 647 (Invitrogen, CA) and Goat anti-Mouse IgG AF 555(Invitrogen, CA). Immunostaining for bovine cartilage was conducted using the same procedure described above.

Biochemical analysis

Biochemical analysis was conducted as described previously[52]. Briefly, the hydrogels containing chondrocytes were removed from their culture medium. The gels were frozen and lyophilized. The dry mass of gel was measured as the mass of the lyophilized constructs. Then the gels were digested in DPBS containing papainase (Worthington, NJ) at 60°C for 16 hours. The PicoGreen assay (Molecular Probes, OR) was utilized to measure amount of DNA in gels. Lambda phage DNA was used as the standard for DNA quantity with the assay. The 1,9- dimethylmethylene blue (DMMB) assay was conducted to measure the amount of sGAG in hydrogel construct. Shark chondroitin sulfate (Sigma, MO) was used as the standard of sGAG amount under the DMMB assay[53,54]. The hydroxyproline assay was applied to measure the amount of collagen contents in gels after acid hydrolysis[55]. Hydroxy-L-proline (Sigma, MO) was used as the standard of hydroxyproline amount under the assay. Collagen amount was converted from hydroxyproline amount with a 1:7.46 hydroxyproline:collagen mass ratio[55]. Values reported for sGAG, collagen, and DNA were normalized with the dry mass of gel.

Level of cell death with LDH assay

For assessing the level of cell death in each of the gels, the release of the intracellular enzyme lactate dehydrogenase (LDH) into the cell culture media was measured with the Promega CytoTox fluorescence assay kit (Promega, CA), using an LDH standard and according to the manufacturer's instruction. Briefly, 10μl of culture medium at each time point (day 2, 4, and 7) was added into a 96 well plate (Corning, MA), and diluted substrate solution was then mixed with the culture medium. The resulting mix was incubated in the dark for 1 hour. Absorbance values at 560nm were measured using a plate reader (Bio Tek, VT). The amounts of LDH were normalized by the value of LDH leased from cells encapsulated in the hydrogels with the slowest stress relaxation.

IL-1β secretion analysis

The gels containing chondrocytes were removed from culture medium after 7 days of culture and washed in DPBS. Gels were then crushed with RNase free pestles (Fisher, PA) for homogenization in a microcentrifuge tube (Corning, MA). The crushed gels were then totally disassociated by adding 5 mM EDTA solution, composed of sodium phosphate dibasic (Na_2HPO_4, Sigma, MO) and ethylenediaminetetraacetic acid disodium salt dehydrate (Na_2EDTA, Sigma, MO). The solution was centrifuged at 10,000 rpm for 5 minutes and the supernatant was extracted. The protein concentration of IL-1β in the supernatant was quantified using the bovine IL-1β ELISA Reagent Kit (Thermofisher, MA), with recombinant bovine IL-1β as a standard, and according to the manufacturer's instruction. The measured values were normalized to DNA amounts in each of the gels.

Gene expression analysis

TRIZOL (Invitrogen, CA) and the total RNA extraction kit (Epoch, TX) were used to harvest RNA in each of the cell-gel constructs and in bovine cartilage. Polymerase chain reaction (PCR) with a High-Capacity cDNA Reverse Transcription Kit (Thermofisher, MA) was conducted to transcribe 300 ng of RNA extracted from each sample into cDNA. Levels

of gene expression was measured with Real time PCR using Fast SYBR green master mix (Applied Biosystems, CA) and bovine specific primers (Table S1). Relative gene expression was quantified using $2^{-\Delta;\Delta Ct}$ method and internally normalized to beta-actin and then compared to isolated primary chondrocytes. Used anabolic genes were Type II collagen (COL2), aggrecan (AGGRECAN), type I collagen (COL1), and type X collagen, and catabolic genes were MMP13 and ADAMTS4. Gene expressions of IL-1β and Sox9 were also quantified with the same method.

Image analysis

For assessing proliferation, immunohistochemical stainings of cells for DAPI/phalloidin/KI-67 were imaged using a Leica confocal microscope with a 64X NA = 1.40 PlanApo oil immersion objective. The proliferation rate of chondrocytes was then calculated by manually counting the number of cells with a nucleus staining positive for Ki67 among a random selection of 300 cells. For quantification of area of cartilage matrix per cell or single cell area in an image, the area stained with a type II collagen antibody in 6 different sections obtained from 3 independent gels was measured as a proxy for cartilage matrix area, while the area stained with phalloidin was measured to determine cell area, using a custom routine in Image J. Then both areas were normalized by the number of nuclei counted in the image of the DAPI channel.

Inhibition of IL-1 signaling

After encapsulation of chondrocytes in slow relaxing gels that exhibited an initial modulus as 3kPa, cell-gel constructs were placed in culture media with 500 ng/ml bovine IL-1Ra (Innovative Research, MI). The concentration of IL-1Ra was determined from our own pilot studies and the value is comparable to that used for a similar purpose in another study[56,57]. Levels of LDH and gene expression of MMP13 and ADAMTS4 were measured as described above after seven days of culture.

Osmotic pressure studies

To modulate osmotic pressure in the culture medium, 400 Da polyethylene glycol (PEG 400, TCI America, MA) was added to the culture media in different amounts, as done previously[58,59]. Briefly, different concentrations of sterilized PEG 400 were added to culture media following encapsulation of chondrocytes into gels with a relaxation time of 436 seconds with an initial modulus of 3kPa. Concentrations of 0% (control), 2%, 4%, and 8% by wt/vol of PEG 400 were added to the media for the experiments. Osmotic pressures were determined from these concentrations using the empirically determined formula[55]: $y = 0.00002c^4 - 0.0007c^3 + 0.0311c^2 + 0.5596c$ as c indicates concentration of PEG 400 in media. After 7 days of culture, immunohistochemical staining was performed and then image analysis was conducted to measure cell size as described above. Proliferation of cells, levels of cell death, and relative expression of MMP13, ADAMTS4 and IL-1β were measured as described above.

Statistical analysis

All experiments were conducted using at least three replicate hydrogels per condition. Statistical analyses were performed using one- or two-way analysis of variance (ANOVA) with post hoc Bonferroni's multiple comparison test used to make pairwise comparisons between multiple groups or a two-tailed student t-test when only two groups were being compared using GraphPad Prism 7.0 statistical software (GraphPad Software). Trends were evaluated for statistical significance with Spearman's rank correlation test, also using GraphPad Prism. Differences were considered to be statistical significant when $p<0.05$. Data are expressed as means ± s.e.m., with n denoting the number of samples analyzed or with box and whisker plots, which show 25/50/75th percentiles as box plots and whiskers as minimum/maximum. F-values and degrees of freedom for all ANOVAs, and t-values and degree of freedom for all t-tests, are provided in Supplementary Table 3.

Supplementary Material

Refer to Web version on PubMed Central for supplementary material.

Acknowledgments

The authors acknowledge the help of Ryan Stowers, Joanna Lee, Albert Arvayo, Janice Lai, Gaby Baylon, Mousavi Aliyeh, Katrina Wisdom, Sungmin Nam, Soah Lee, Dayoon No, Jungho Yu, Kyuwon Kim, Kyuho Han and all members of the Chaudhuri lab, and thank David Weitz (Harvard University) for helpful discussions. This work was supported by the Jeongsong Cultural Foundation (to H.L.), NIH grant R01 DE013033 (to D.M.), and DARPA grant D14AP00044 (to O.C.).

References

1. Getgood A, Brooks R, Fortier L, Rushton N. Articular cartilage tissue engineering: today's research, tomorrow's practice? J Bone Joint Surg Br. 2009; 91:565–576. [PubMed: 19407287]
2. Guettler JH. Osteochondral Defects in the Human Knee: Influence of Defect Size on Cartilage Rim Stress and Load Redistribution to Surrounding Cartilage. Am J Sports Med. 2004; 32:1451–1458. [PubMed: 15310570]
3. Brittberg M, Lindahl A, Nilsson A, Ohlsson C, Isaksson O, Peterson L. Treatment of deep cartilage defects in the knee with autologous chondrocyte transplantation. J Med. 1994; 331:889–895.
4. Gibson AJ, McDonnell SM, Price AJ. Matrix-Induced Autologous Chondrocyte Implantation. Oper Tech Orthop. 2006; 16:262–265.
5. Steadman JR, Rodkey WG, Briggs KK, Rodrigo JJ. The microfracture technic in the management of complete cartilage defects in the knee joint. Orthopade. 1999; 28:26–32. [PubMed: 10081041]
6. Görtz S, Bugbee WD. Allografts in articular cartilage repair. Instr Course Lect. 2007; 56:469–480. [PubMed: 17472329]
7. Roberts S, Menage J, Sandell LJ, Evans EH, Richardson JB. Immunohistochemical study of collagen types I and II and procollagen IIA in human cartilage repair tissue following autologous chondrocyte implantation. Knee. 2009; 16:398–404. [PubMed: 19269183]
8. Gobbi A, Nunag P, Malinowski K. Treatment of full thickness chondral lesions of the knee with microfracture in a group of athletes. Knee Surgery, Sport Traumatol Arthrosc. 2005; 13:213–221.
9. Lee CSD, Gleghorn JP, Won Choi N, Cabodi M, Stroock AD, Bonassar LJ. Integration of layered chondrocyte-seeded alginate hydrogel scaffolds. Biomaterials. 2007; 28:2987–2993. [PubMed: 17382380]
10. Lima EG, Bian L, Ng KW, Mauck RL, Byers Ba, Tuan RS, Ateshian Ga, Hung CT. The beneficial effect of delayed compressive loading on tissue-engineered cartilage constructs cultured with TGF-β3. Osteoarthr Cartil. 2007; 15:1025–1033. [PubMed: 17498976]

11. Mauck RL, Soltz Ma, Wang CC, Wong DD, Chao PH, Valhmu WB, Hung CT, Ateshian Ga. Functional tissue engineering of articular cartilage through dynamic loading of chondrocyte-seeded agarose gels. J Biomech Eng. 2000; 122:252–260. [PubMed: 10923293]
12. Bryant SJ, Anseth KS. Hydrogel properties influence ECM production by chondrocytes photoencapsulated in poly(ethylene glycol) hydrogels. J Biomed Mater Res. 2002; 59:63–72. [PubMed: 11745538]
13. Schuh E, Hofmann S, Stok K, Notbohm H, Müller R, Rotter N. Chondrocyte redifferentiation in 3D: The effect of adhesion site density and substrate elasticity. J Biomed Mater Res - Part A. 2012; 100 A:38–47.
14. Burdick JA, Chung C, Jia X, Randolph MA, Langer R. Controlled degradation and mechanical behavior of photopolymerized hyaluronic acid networks. Biomacromolecules. 2005; 6:386–391. [PubMed: 15638543]
15. Mouw JK, Case ND, Guldberg RE, Plaas AHK, Levenston ME. Variations in matrix composition and GAG fine structure among scaffolds for cartilage tissue engineering. Osteoarthr Cartil. 2005; 13:828–836. [PubMed: 16006153]
16. Francioli SE, Candrian C, Martin K, Heberer M, Martin I, Barbero A. Effect of three-dimensional expansion and cell seeding density on the cartilage-forming capacity of human articular chondrocytes in type II collagen sponges. J Biomed Mater Res - Part A. 2010; 95:924–931.
17. Erickson IE, Kestle SR, Zellars KH, Farrell MJ, Kim M, Burdick JA, Mauck RL. High mesenchymal stem cell seeding densities in hyaluronic acid hydrogels produce engineered cartilage with native tissue properties. Acta Biomater. 2012; 8:3027–3034. [PubMed: 22546516]
18. Chaudhuri O, Gu L, Klumpers D, Darnell M, Bencherif SA, Weaver JC, Huebsch N, Lee HP, Lippens E, Duda GN, Mooney DJ. Hydrogels with tunable stress relaxation regulate stem cell fate and activity. Nat Mater. 2015; 15:326–333. [PubMed: 26618884]
19. McKinnon DD, Domaille DW, Cha JN, Anseth KS. Biophysically defined and cytocompatible covalently adaptable networks as viscoelastic 3d cell culture systems. Adv Mater. 2014; 26:865–872. [PubMed: 24127293]
20. Nicodemus GD, Skaalure SC, Bryant SJ. Gel structure has an impact on pericellular and extracellular matrix deposition, which subsequently alters metabolic activities in chondrocyte-laden PEG hydrogels. Acta Biomater. 2011; 7:492–504. [PubMed: 20804868]
21. Lin S, Sangaj N, Razafiarison T, Zhang C, Varghese S. Influence of physical properties of biomaterials on cellular behavior. Pharm Res. 2011; 28:1422–1430. [PubMed: 21331474]
22. Chung C, Mesa J, Randolph MA, Yaremchuk M, Burdick JA. Influence of gel properties on neocartilage formation by auricular chondrocytes photoencapsulated in hyaluronic acid networks. J Biomed Mater Res Part A. 2006; 77A:518–525.
23. Lee KY, Mooney DJ. Hydrogels for tissue engineering. Chem Rev. 2001; 101:1869–1879. [PubMed: 11710233]
24. Guo JF, Jourdian GW, MacCallum DK. Culture and growth characteristics of chondrocytes encapsulated in alginate beads. Connect Tissue Res. 1989; 19:277–97. [PubMed: 2805684]
25. Mhanna R, Kashap A, Palazzolo G, Vallmajo-Martin Q, Becher J, Möller S, Schnabelrauch M, Zenobi-Wong M. Chondrocyte Culture in 3D Alginate Sulfate Hydrogels Promotes Proliferation While Maintaining Expression of Chondrogenic Markers. Tissue Eng Part A. 2013; 20:1–38. [PubMed: 23924293]
26. Beekman B, Verzijl N, Bank RA, von der Mark K, TeKoppele JM. Synthesis of collagen by bovine chondrocytes cultured in alginate; posttranslational modifications and cell-matrix interaction. Exp Cell Res. 1997; 237:135–41. [PubMed: 9417876]
27. Chaudhuri O, Gu L, Darnell M, Klumpers D, Bencherif SA, Weaver JC, Huebsch N, Mooney DJ. Substrate stress relaxation regulates cell spreading. Nat Commun. 2015; 6:6364.
28. Zhao X, Huebsch N, Mooney DJ, Suo Z. Stress-relaxation behavior in gels with ionic and covalent crosslinks. J Appl Phys. 2010; 107:1–5.
29. Wilusz RE, Sanchez-Adams J, Guilak F. The structure and function of the pericellular matrix of articular cartilage. Matrix Biol. 2014; 39:25–32. [PubMed: 25172825]
30. Schuh E, Hofmann S, Stok KS, Notbohm H, Müller R, Rotter N. The influence of matrix elasticity on chondrocyte behavior in 3D. J Tissue Eng Regen Med. 2012; 6:31–42.

31. Lefrebvre V, de Crombrugghe B. Toward understanding S0X9 function in chondrocyte differentiation. Matrix Biol. 1998; 16:529–540. [PubMed: 9569122]
32. Sandell LJ, Aigner T. Articular cartilage and changes in Arthritis: Cell biology of osteoarthritis. Arthritis Res. 2001; 3:107. [PubMed: 11178118]
33. Daheshia M, Yao JQ. The interleukin 1beta pathway in the pathogenesis of osteoarthritis. J Rheumatol. 2008; 35:2306–2312. [PubMed: 18925684]
34. Pelletier JP, DiBattista JA, Roughley P, McCollum R, Martel-Pelletier J. Cytokines and inflammation in cartilage degradation. Rheum Dis Clin North Am. 19:545–568.
35. Buckwalter, Ja, Mower, D., Ungar, R., Schaeffer, J., Ginsberg, B. Morphometric analysis of chondrocyte hypertrophy. J Bone Joint Surg Am. 1986; 68:243–55. [PubMed: 3944163]
36. Desrochers J, Amrein MW, Matyas JR. Viscoelasticity of the articular cartilage surface in early osteoarthritis. Osteoarthr Cartil. 2012; 20:413–421. [PubMed: 22313971]
37. Guilak F, Alexopoulos L, Nielsen R, Ting-Beall HP, Haider M. The biomechanical properties of the chondrocyte pericellular matrix: micropipette aspiration of mechanically isolated chondrons. Trans Annu Meet Res Soc. 2002:404–405.
38. Nguyen BV, Wang QG, Kuiper NJ, El Haj AJ, Thomas CR, Zhang Z. Biomechanical properties of single chondrocytes and chondrons determined by micromanipulation and finite-element modelling. J R Soc Interface. 2010; doi: 10.1098/rsif.2010.0207
39. Leipzig ND, Athanasiou KA. Unconfined creep compression of chondrocytes. J Biomech. 2005; 38:77–85. [PubMed: 15519342]
40. Darling EM, Zauscher S, Guilak F. Viscoelastic properties of zonal articular chondrocytes measured by atomic force microscopy. Osteoarthr Cartil. 2006; 14:571–579. [PubMed: 16478668]
41. Wong M, Siegrist M, Wang X, Hunziker E. Development of mechanically stable alginate/chondrocyte constructs: Effects of guluronic acid content and matrix synthesis. J Orthop Res. 2001; 19:493–499. [PubMed: 11398865]
42. Cooper KL, Oh S, Sung Y, Dasari RR, Kirschner MW, Tabin CJ. Multiple phases of chondrocyte enlargement underlie differences in skeletal proportions. Nature. 2013; 495:375–8. [PubMed: 23485973]
43. Bush PG, Hall AC. The volume and morphology of chondrocytes within non-degenerate and degenerate human articular cartilage. Osteoarthr Cartil. 2003; 11:242–251. [PubMed: 12681950]
44. O'Conor CJ, Leddy HA, Benefield HC, Liedtke WB, Guilak F. TRPV4-mediated mechanotransduction regulates the metabolic response of chondrocytes to dynamic loading. Proc Natl Acad Sci U S A. 2014; 111:1316–21. [PubMed: 24474754]
45. Discher DE, Janmey P, Wang YL. Tissue cells feel and respond to the stiffness of their substrate. Science. 2005; 310:1139–43. [PubMed: 16293750]
46. Huebsch N, Arany PR, Mao AS, Shvartsman D, Ali OA, Bencherif SA, Rivera-Feliciano J, Mooney DJ. Harnessing traction-mediated manipulation of the cell/matrix interface to control stem-cell fate. Nat Mater. 2010; 9:518–26. [PubMed: 20418863]
47. Vogel V, Sheetz M. Local force and geometry sensing regulate cell functions. Nat Rev Mol Cell Biol. 2006; 7:265–275. [PubMed: 16607289]
48. Khetan S, Guvendiren M, Legant WR, Cohen DM, Chen CS, Burdick Ja. Degradation-mediated cellular traction directs stem cell fate in covalently crosslinked three-dimensional hydrogels. Nat Mater. 2013; 12:458–65. [PubMed: 23524375]
49. Nicodemus GD, Bryant SJ. Cell Encapsulation in Biodegradable Hydrogels for Tissue Engineering Applications. Tissue Eng Part B Rev. 2008; 14:149–165. [PubMed: 18498217]
50. Kim JH, Lee G, Won Y, Lee M, Kwak JS, Chun CH, Chun JS. Matrix cross-linking-mediated mechanotransduction promotes posttraumatic osteoarthritis. Proc Natl Acad Sci U S A. 2015; 112:9424–9. [PubMed: 26170306]
51. Nam S, Hu KH, Butte MJ, Chaudhuri O. Strain-enhanced stress relaxation impacts nonlinear elasticity in collagen gels. Proc Natl Acad Sci. 2016; 113:201523906.
52. Lai JH, Kajiyama G, Smith RL, Maloney W, Yang F. Stem cells catalyze cartilage formation by neonatal articular chondrocytes in 3D biomimetic hydrogels. Sci Rep. 2013; 3:3553. [PubMed: 24352100]

53. Farndale RW, Buttle DJ, Barrett AJ. Improved quantitation and discrimination of sulphated glycosaminoglycans by use of dimethylmethylene blue. BBA - Gen Subj. 1986; 883:173–177.

54. Enobakhare BO, Bader DL, Lee Da. Quantification of sulfated glycosaminoglycans in chondrocyte/alginate cultures, by use of 1,9-dimethylmethylene blue. Anal Biochem. 1996; 243:189–191. [PubMed: 8954546]

55. Stegemann H, Stalder K. Determination of hydroxyproline. Clin Chim Acta. 1967; 18:267–273. [PubMed: 4864804]

56. Im HJ, Pacione C, Chubinskaya S, Van Wijnen AJ, Sun Y, Loeser RF. Inhibitory Effects of Insulin-like Growth Factor-1 and Osteogenic Protein-1 on Fibronectin Fragment- and Interleukin-1β-stimulated Matrix Metalloproteinase-13 Expression in Human Chondrocytes. J Biol Chem. 2003; 278:25386–25394. [PubMed: 12734180]

57. Smith LJ, Chiaro JA, Nerurkar NL, Cortes DH, Horava SD, Hebela NM, Mauck RL, Dodge GR, Elliott DM. Nucleus pulposus cells synthesize a functional extracellular matrix and respond to inflammatory cytokine treatment following long term agarose culture. Eur Cells Mater. 2011; 20:291–301.

58. Lagerwerff JV, Ogata G, Eagle HE. Control of Osmotic Pressure of Culture Solutions with Polyethylene Glycol. Science (80-). 1961; 133:1486–1487.

59. Stanley CB, Strey HH. Measuring osmotic pressure of poly(ethylene glycol) solutions by sedimentation equilibrium ultracentrifugation. Macromolecules. 2003; 36:6888–6893.

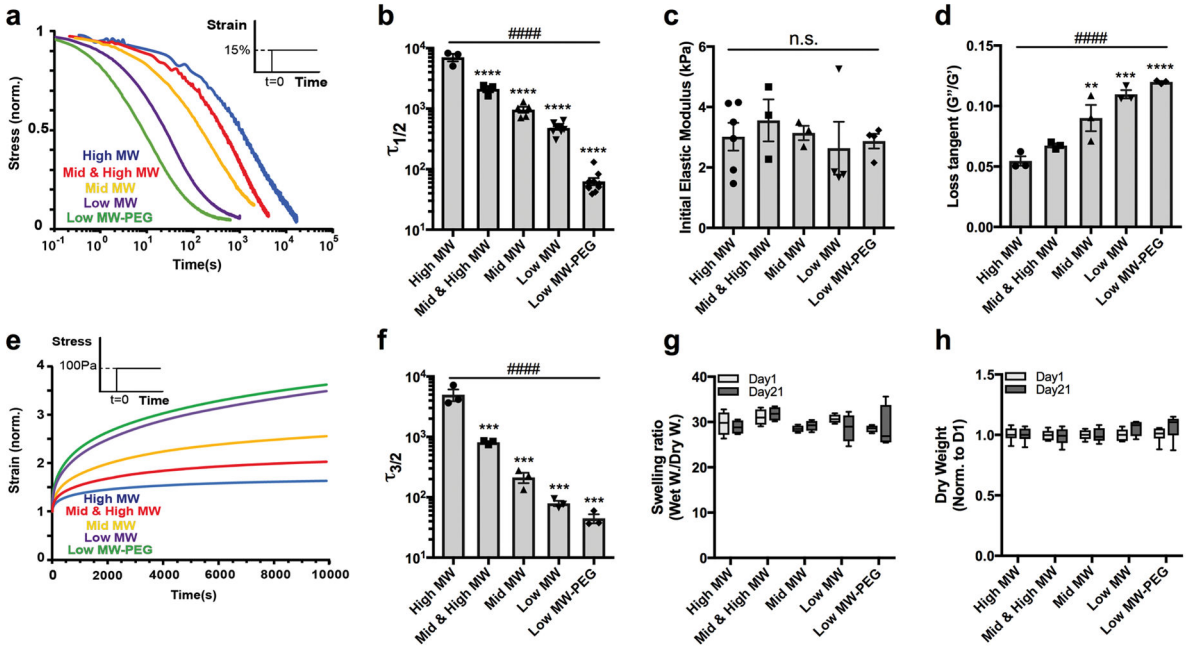

Figure 1. Modulating the rate of stress relaxation or creep of alginate hydrogels independent of initial elastic modulus, swelling, and degradation

a, Representative stress relaxation profiles of alginate hydrogels composed of alginate of varying molecular weights, or modified with a short PEG spacer. **b**, Time scale of stress relaxation, $\tau_{1/2}$, for the different alginate hydrogels. **c**, Initial elastic modulus of the different alginate hydrogels. (p=0.2818 by Spearman's rank correlation, and $p > 0.7407$ by one-way ANOVA test). **d**, Quantification of the loss tangent for the different alginate hydrogel formulations. **e**, Representative creep profiles of the different alginate hydrogels. **f**, Time scale of creep response, $\tau_{3/2}$, for the different alginate hydrogels. **g**, Swelling ratio of alginate hydrogels were measured after 1 day or 21 days in culture. ($p > 0.9999$ for both time points by two-way ANOVA test, and $p > 0.2$ for each hydrogel at different time points by Student's t test). **h**, Dry mass of alginate hydrogels after 1 day or 21 days in culture normalized by the value at day 1. ($p > 0.9999$ for both time points by two-way ANOVA test, and $p > 0.2661$ for each hydrogel at different time points by student's t test). #### located on the top indicates $p < 0.0001$ by Spearman's rank correlation. **, ***, and **** indicate a statistically significant difference when compared to high MW alginate condition with $p <$ 0.01, 0.001, and 0.0001 by one-way ANOVA test. All data are shown as mean ± s.e.m, n≥ 3 replicates per conditions, except for g and h, which show 25/50/75th percentiles as box plots and whiskers as minimum/maximum.

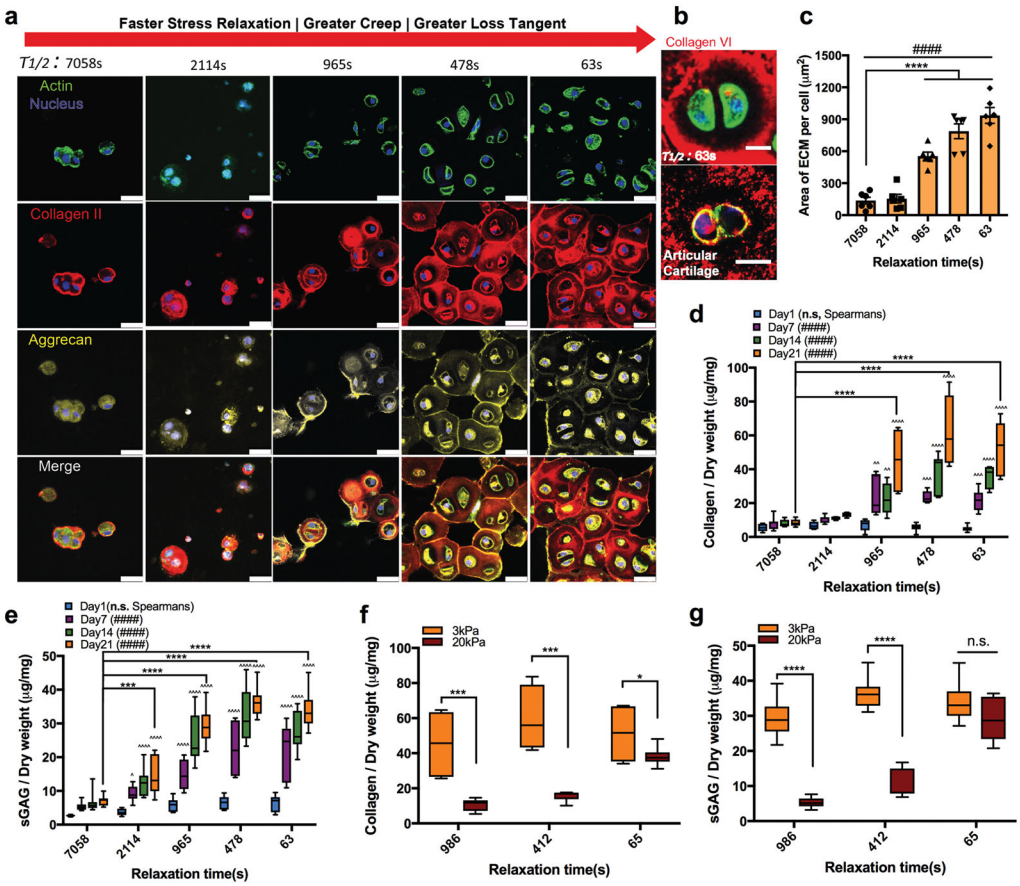

Figure 2. Faster stress relaxation in the hydrogels promotes increased cartilage matrix production and formation of a wider volume of interconnected cartilage matrix

a, Immunohistochemical stains of chondrocytes cultured in 3kPa hydrogels for 21 days. Scale bar, 25 μm. **b**, Immunohistochemical stains of pericellular matrix and bean-shaped chondrocytes cultured in fast relaxing gel ($\tau_{1/2}$ = 63s) for 21 days and in hyaline cartilage. Scale bar, 10 μm. **c**, Quantification of area of type II collagen per cell constructed by chondrocytes for 21 days. (n = 6 images from 3 hydrogels per each condition, #### $p <$ 0.0001 by Spearman's rank correlation, **** $p < 0.0001$ compared to the slow relaxing gel ($\tau_{1/2}$ = 7058s) condition by one-way ANOVA test, mean ± s.e.m.). **d–e**, Quantification of accumulated (d) collagen and (e) sulfated glycosaminoglycan (sGAG) produced by chondrocytes cultured for 21 days (#### $p < 0.0001$ by Spearman's rank correlation; *** $p <$ 0.001, and **** $p < 0.0001$ compared to slow relaxing gel ($\tau_{1/2}$ =7058s) condition by one-way ANOVA test). **f–g**, Quantification of the accumulated (f) collagen and (g) sGAG after 21 days in 3 kPa or 20 kPa alginate gels (*$p < 0.05$, *** $p < 0.001$ and **** $p < 0.0001$ by student's t-test). The box plots show 25/50/75th percentiles and whiskers show minimum/ maximum. Biological replicates (n = 4) are represented in **d**–**g**.

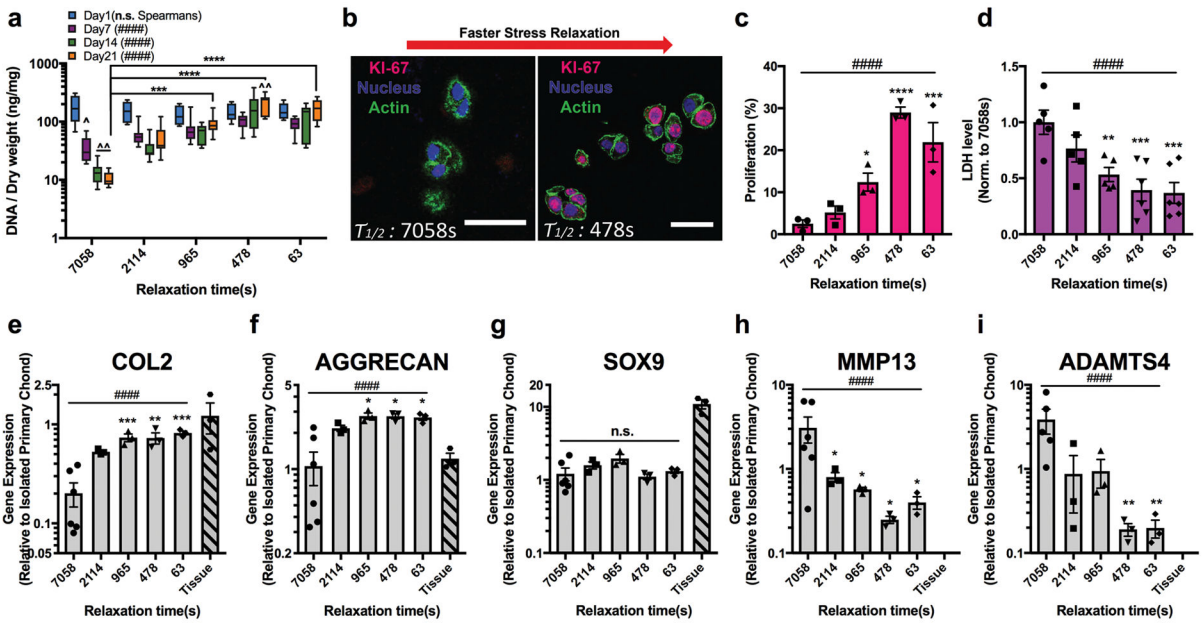

Figure 3. Faster relaxation promotes proliferation and anabolic, or matrix forming, gene expression in chondrocytes, while slower stress relaxation induces cell death and catabolic, or matrix degrading, gene expression in chondrocytes

a, Quantification of DNA content in constructs consisting of chondrocytes cultured in 3 kPa hydrogels over 21 days (n=4 biological replicates, ^ p <0.05, and ^^ p <0.01 compared to value at Day 1 by two-way ANOVA test). The box plots show 25/50/75th percentiles and whiskers show minimum/maximum. **b**, Immunohistochemical stains for Ki-67 in nucleus of chondrocytes cultured for 7 days. Scale bar, 25 μm. **c**, Quantification of chondrocyte proliferation (n=3 biological replicates, measured in 200+ cells per replicate). **d**, Quantification of LDH levels after 7 days of culture, normalized by the value in the slowest relaxing gel condition (n=5 replicates per conditions). **e–g**, Quantification of gene expression of (e) type II collagen (COL2), (f) aggrecan (AGGRECAN), (g) the transcription factor Sox9 (SOX9), (h) a collagenase (MMP13), and (i) an aggrecanase (ADAMTS4) after 7 days of culture (n=3 replicates per conditions). Values are normalized by gene expression levels measured in isolated primary chondrocytes, and gene expression of chondrocytes in articular cartilage are indicated by the label “tissue”. *, **, ***, and **** indicate statistical significant difference when value compared to that in the slowest relaxing gel condition with p <0.05, 0.01, 0.001, and 0.0001 respectively (two-way ANOVA test in **a** and one-way ANOVA test in **c**–**i**). ### and #### on the top in each figure indicate p <0.001 and 0.0001 respectively (Spearman’s rank correlation). Data are shown as mean ± s.e.m. in **c**–**i**.

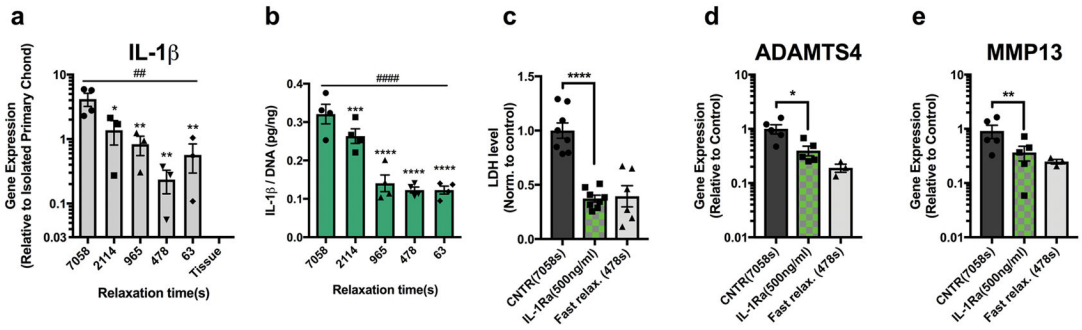

Figure 4. Slower stress relaxation induces secretion of IL-1β, which mediates strong up-regulation of catabolic activities of chondrocytes and cell death

a, Quantification of gene expression of IL-1β for chondrocytes after 7 days. Values are normalized by the gene expression level measured in isolated primary chondrocytes, and gene expression of chondrocytes in articular cartilage are indicated by the label "tissue". (n≥ 3 replicates per conditions, ## $p < 0.01$ by Spearman's rank correlation). **b**, Quantification of the amount of IL-1β secreted into the hydrogels after 7 days of culture in the indicated conditions, normalized to DNA amounts (n=4 replicates per conditions, #### $p < 0.0001$ by Spearman's rank correlation). From **a** to **b**, *, **, ***, and **** indicate a statistically significant difference when compared to slowest relaxing gel condition ($\tau_{1/2}$=7058s) with $p < 0.05$, 0.01, 0.001 and 0.0001 respectively (one-way ANOVA test). **c**, LDH levels in media for chondrocytes cultured in the slowest relaxing gel in the presence (IL-1Ra) or absence (CNTR) of IL-1Ra, normalized by the value for the control group (n=8 replicates per conditions). LDH level in media for chondrocytes cultured in faster relaxing gels ($\tau_{1/2}$=478s) is shown for comparison. **d–e**, Relative gene expression of MMP13 and ADAMTS4 in the presence (IL-1Ra) or absence (CNTR) of IL-1Ra (n=3 replicates per conditions). Gene expression levels for chondrocytes cultured in faster relaxing gels (478s) are shown for comparison. From **c** to **e**, *, ** and **** indicate statistical significant difference when compared to control (7058s) with $p < 0.05$, 0.01 and 0.0001 respectively (Student's *t*-test). All data are shown as mean ± s.e.m.

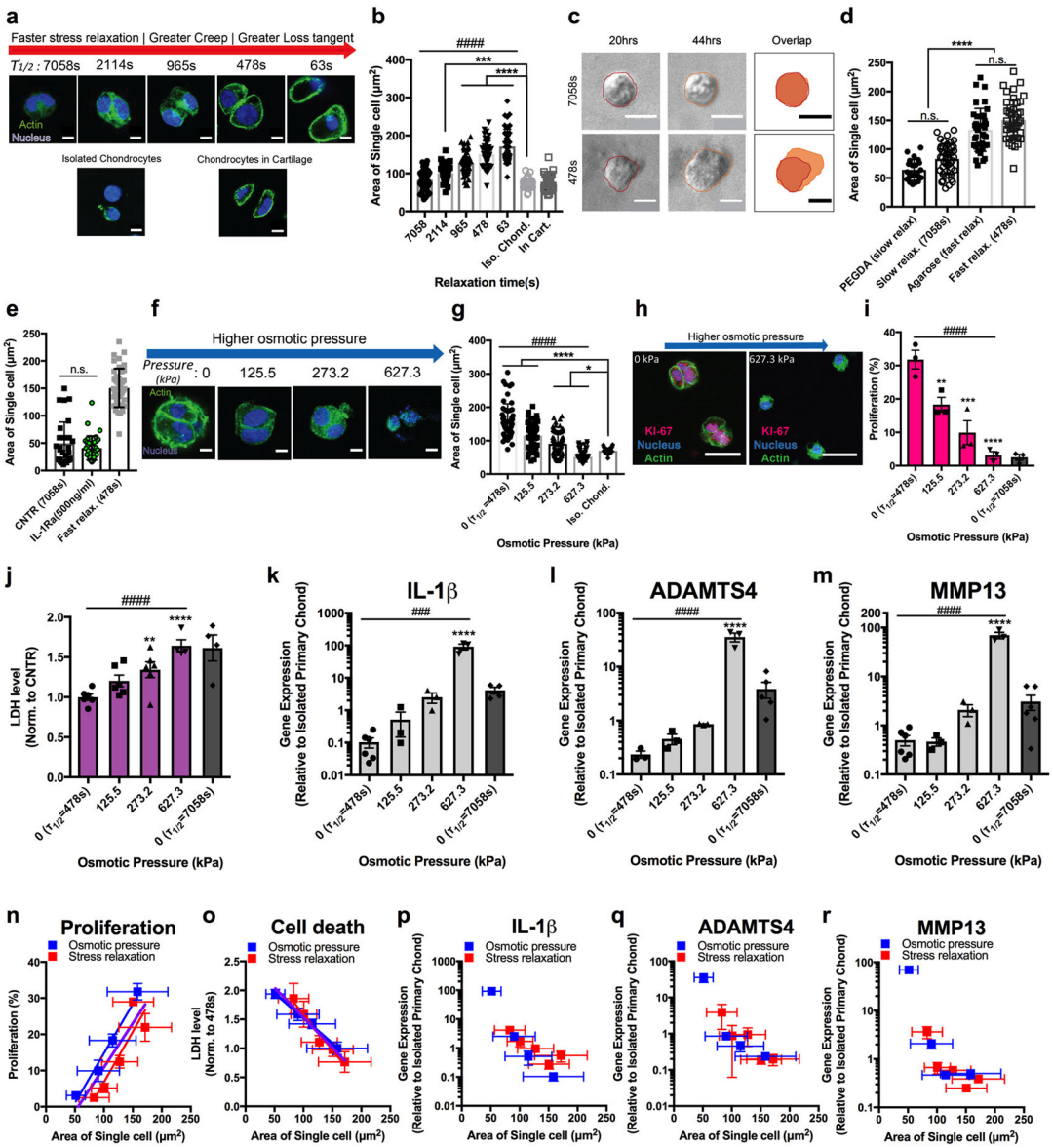

Figure 5. Spatial confinement against cell expansion in hydrogels with slow stress relaxation induces decreased proliferation and increases in IL-1β secretion, cell death and catabolic activities of cells

a, Chondrocytes after 7 days. Scale bar, 5μm. **b**, Chondrocyte size (n > 50, #### $p < 0.0001$, Spearman's correlation, *** $p < 0.001$, and **** $p < 0.0001$, one-way ANOVA). **c**, Timelapse images of chondrocytes. Scale bar, 10 μm. **d**, Chondrocyte size in PEG and agarose hydrogels (n > 25 cells, $p < 0.0001$, one-way ANOVA), compared to alginate hydrogels (n.s. $p > 0.09$, one-way ANOVA). **e**, Chondrocyte size in slow relaxing hydrogels in absence (CNTR) or presence of IL-1Ra (n > 30, p=0.27, t-test). **f**, Chondrocytes in fast relaxing gels after 7 days. Scale bar, 5μm. **g**, Chondrocyte size (n > 50 cells, #### p <0.0001, Spearman's correlation, * and **** indicate $p < 0.05$ or 0.0001, one-way ANOVA). **h**, Ki-67 stainings. Scale bar, 25 μm. **i**, Chondrocyte proliferation (n=3, 200+ cells per replicate, #### $p < 0.0001$, Spearman's correlation). **j**, Normalized LDH levels (n=5,

Spearman's rank correlation, p <0.0001). **k–m**, Normalized gene expression of (k) IL-1β, (l) MMP13, and (m) ADAMTS4 after 7 days of culture (n=3, ### p <0.001, and #### p <0.0001, Spearman's correlation). From **k** to **m**, *, **, ***, and **** indicate statistical significant difference against control with p <0.05, 0.01, 0.001, and 0.0001 respectively (one-way ANOVA). **n–r,** Scatter plots of (n) proliferation, (o) LDH levels, and gene expression of (p) IL-1β, (q) MMP13, and (r) ADAMTS4 with cell area for varying stress relaxation or osmotic pressure. For **n** and **o**, linear regression analysis showed a global trend (purple line) of proliferation or cell death with area of single cells. Data are shown as mean ± s.e.m.

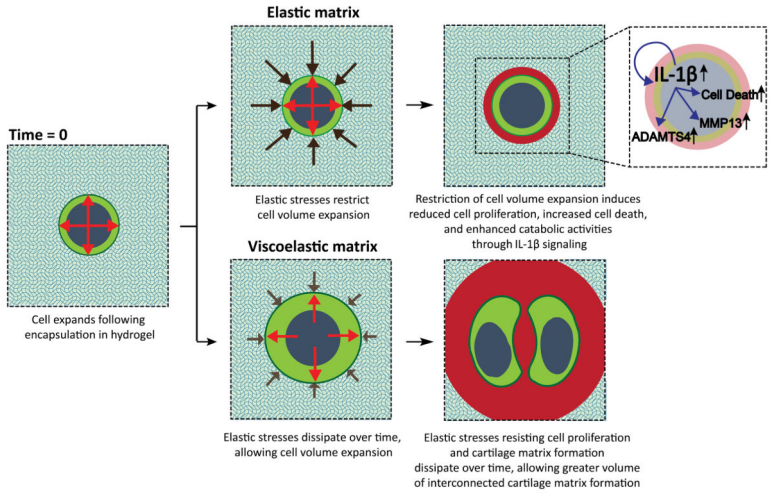

Figure 6. Hydrogel stress relaxation regulates chondrocyte phenotype through restricting cell volume expansion and cartilage matrix formation

Primary chondrocytes initially expand their volume following encapsulation in a hydrogel. In an elastic hydrogel, elastic stresses from the solid matrix resist the expansion and confine cell volume. Spatial confinement of cell volume inhibits proliferation of the cell and stimulates production of IL-1β, which in turn drives catabolic activities of chondrocytes and cell death. In a viscoelastic hydrogel with fast stress relaxation, elastic stresses are dissipated over time, allowing cell volume expansion. Over longer times, elastic stresses resisting cell proliferation and cartilage matrix deposition are also relaxed, allowing formation of a greater volume of interconnected cartilage matrix.